3D-shortest paths for a hypersonic glider in a heterogeneous environment

Pawit Pharpatara, Bruno Hérissé, Yasmina Bestaoui

3D-shortest paths for a hypersonic glider in a heterogeneous environment

Pawit Pharpatara * **Bruno Hérissé** * **Yasmina Bestaoui** **

* *Onera - The French Aerospace Lab, Palaiseau, France (email: pawit.pharpatara@onera.fr, bruno.herisse@onera.fr.)*
** *IBISC, Université d'Evry-Val-d'Essonne, Evry, France (e-mail: Yasmina.Bestaoui@ufrst.univ-evry.fr).*

Abstract: Shortest paths in 3-dimensional space of a hypersonic glider in a heterogeneous environment are considered in this paper. The environment is heterogeneous in the sense that the maximum curvature of the vehicle path varies and depends on the position of the vehicle. Path generation is based on the Dubins-like model. It assumes that initial and final states are sufficiently far from each other so that the CSC (Curve-Straight line-Curve) path is the shortest path between both states. Paths are calculated based on the optimal control theory and a geometrical approach. This method is computationally fast and easy to implement in a real time system. Moreover, paths found by this method are more realistic than existing Dubins' paths.

Keywords: Aerospace trajectories, optimal trajectories, autonomous vehicle, trajectory planning, aerospace control.

1. INTRODUCTION

The purpose of this paper is to generate the shortest path in 3-dimensional space for an aerial vehicle flying in a heterogeneous environment where the maximum curvature of the path varies in the environment. In case of aerial vehicles, the maximum curvature of the path that the vehicle can perform depends on the vehicle position. Unmanned aerial vehicles are mostly subjected to aerodynamic forces to maneuver. Moreover, the aerodynamic forces, *i.e.* lift (f_L) and drag (f_D), depend on aerodynamic coefficients (C_L and C_D), surface of reference (S), vehicle speed (v) and air density ($\rho(z)$).

$$f_L = \frac{1}{2}\rho(z)SC_Lv^2$$
$$f_D = \frac{1}{2}\rho(z)SC_Dv^2$$

Thus, the maneuverability, *i.e.* maximum curvature, of the aerial vehicles depends on the air density which decreases exponentially with altitude z (see Section 2.1).

The shortest path between two vehicle states is a key element in many planning algorithms. In a 2-dimensional plane, the shortest path of Dubins' vehicle is usually used to determine the distance between two states. The study was initiated and solved geometrically in Dubins (1957) with a vehicle only moving forward. In his study, a vehicle with constant turning radius was used. Dubins stated that the shortest path between initial and final states was a combination of straight lines (S) and arcs of circle (C), *i.e.* CSC paths, CCC paths or degenerated forms of these. Dubins' work inspired a lot of researchers later on. Reeds and Shepp (1990) extended the study with a vehicle moving forward and backward. Pontryagin's Minimum Principle was used to solve the Dubins' problem in Boissonnat et al. (1991). The study was extended to the unmanned aerial vehicle whose dynamics was the same as the Dubins' vehicle in McGee et al. (2005) by analyzing the effect of constant wind. In Dolinskaya and Maggiar (2012), a vehicle moving in an anisotropic environment, which meant that the minimum turning radius depended on the orientation of the vehicle, was considered. Later, some generalizations of the Dubins' vehicle in a heterogeneous environment were studied. In Sanfelice and Frazzoli (2008), the environment having two different property planes where the vehicle could maneuver with the same turning rate was considered. Then, in Hérissé and Pepy (2013), shortest paths in heterogeneous environments were considered. The environments are heterogeneous in the sense that the maximum curvature of the vehicle path varies and depends on the position of the vehicle.

The study of Dubins' vehicle has also taken a different path into a 3-dimensional space problem. In Sussmann (1995), it was also demonstrated that, for sufficiently close distance between two states, the helicoidal arc could be shorter than the CSC path. Then, it was shown that the shortest path in a 3-dimensional plane was a helicoidal arc, a CSC path, a CCC path or a degenerated form of these Dubins' paths. Later, in Shanmugavel (2007), Dubins' path in 2-dimensional plane was extended to 3-dimensional plane for multiple UAVs path planning. Suboptimal paths of CCSC type were used.

Recently, the shortest path of Dubins' vehicle in 3-dimensional space was studied for a vehicle with a constant turning radius in Hota and Ghose (2010). The shortest Dubins' path was calculated by using a geometrical approach between initial and final states that were sufficiently far

⋆ This paper is a part of PdD thesis supported and financed by Onera the French Aerospace Lab

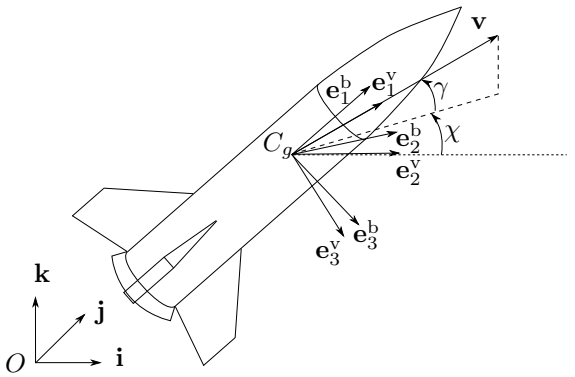

Fig. 1. Vehicle model

from each other so that CSC path was ensured to be the shortest path. Then, a 3-dimensional path generation of the same vehicle model in presence of wind was studied in Hota and Ghose (2014). However, the case studied by Hota and Ghose are mostly for an aerial vehicle flying in low altitude (less than a kilometer). Thus, the maximum curvature of the vehicle path can be considered constant. However, the trajectory found by using Hota's calculation is not applicable for the vehicle flying in a wide range of altitude, *i.e.* the maximum curvature of the vehicle path cannot be considered constant.

In this paper, shortest paths in 3-dimensional space for a hypersonic aerial vehicle flying in a heterogeneous environment are demonstrated. It is assumed that initial and final states are sufficiently far from each other. Thus, the shortest Dubins' path is a CSC path. The calculation is based on the geometrical approach in Hota and Ghose (2010) and the curve (C) generation in Hérissé and Pepy (2013).

This paper is divided into four parts. First, the environment and system models are presented in Section 2. Then, 3-dimensional Dubins' paths in a heterogeneous environment are demonstrated in Section 3. Then, some simulated results are shown and analyzed in Section 4. Finally, some concluding remarks are made in the last section.

2. SYSTEM MODELING

2.1 Environment model

The environment is considered heterogeneous because of variation of air density $\rho(z)$, decreasing exponentially with altitude z. The simplified environment model can be expressed as:

$$\rho(z) = \rho_0 e^{-z/z_r}, \tag{1}$$

where ρ_0 is the air density at standard atmosphere at sea level and z_r is a reference altitude.

2.2 Vehicle model

In this paper, a simplified model of an aerial vehicle is used. It is modeled as a rigid body maneuvering in a 3-dimensional plane. Three frames (Fig. 1) are introduced to describe the motion of the vehicle: an Earth-Centred Earth-Fixed (ECEF) reference frame $\mathcal{I}$ centered at point O and associated with the basis vectors $(\mathbf{i}, \mathbf{j}, \mathbf{k})$; a body-fixed frame $\mathcal{B}$ attached to the vehicle at its center of mass C_g with the vector basis $(\mathbf{e}_1^{\mathrm{b}}, \mathbf{e}_2^{\mathrm{b}}, \mathbf{e}_3^{\mathrm{b}})$; and a velocity frame $\mathcal{V}$ attached to the vehicle at C_g with the vector basis $(\mathbf{e}_1^{\mathrm{v}}, \mathbf{e}_2^{\mathrm{v}}, \mathbf{e}_3^{\mathrm{v}})$ where the translational velocity of the vehicle is denoted $\mathbf{v} = v\mathbf{e}_1^{\mathrm{v}}$ and v is the speed of the vehicle. Position and velocity defined in $\mathcal{I}$ are denoted $\boldsymbol{\xi} = (x, y, z)^\top \in \mathbb{R}^3$ and $\mathbf{v} = (\dot{x}, \dot{y}, \dot{z})^\top \in \mathbb{R}^3$. Denote γ and χ the orientation of the velocity. The flight angle is denoted by γ and the azimuth angle is denoted by χ.

Since it is a simplified model, to eliminate all the external factor to the problem, a zero wind assumption is applied. Then, the translational velocity $\mathbf{v}$ is assumed to coincide with the apparent velocity. Besides, an unpowered hypersonic aerial vehicle such as an interceptor missile during midcourse phase is studied in this paper. Thus, the gravity can be neglected which is a strong hypothesis that is only valid for missile-like aircraft flying in a short distance. Moreover, the drag can be ignored since we are interested in the shortest path between two states, *i.e.* the path of minimum length. Thus, the dynamics of velocity does not need to be considered.

Therefore, the dynamics of a hypersonic aerial vehicle can be written as

$$\begin{cases} \dot{x} = v\cos\gamma\cos\chi, \\ \dot{y} = v\cos\gamma\sin\chi, \\ \dot{z} = v\sin\gamma, \\ \dot{\gamma} = v\dfrac{1}{2m}\rho(z)SC_{L_{\max}}\mu = vc(z)\mu, \\ \dot{\chi} = v\dfrac{1}{2m}\rho(z)SC_{L_{\max}}\dfrac{\eta}{\cos\gamma} = vc(z)\dfrac{\eta}{\cos\gamma}, \end{cases} \tag{2}$$

where μ, η are the normalized control inputs bounded by condition $\sqrt{\mu^2+\eta^2} \leqslant 1$, m is the mass of the vehicle, $\gamma \in [-\pi/2, \pi/2]$, $\chi \in [-\pi, \pi]$, and $c(z) \in \mathbb{R}_+$ is the curvature of the vehicle path. The curvature depends on the altitude of the vehicle z whose maximum value can be written as

$$c(z) = c_0 e^{-z/z_r}. \tag{3}$$

where c_0 is the maximum curvature at sea level.

The optimal control problem consists in minimizing the cost function

$$s_f = \int_0^{t_f} v\, dt \tag{4}$$

where s_f is the final path length and t_f is the final time.

Since we are interested in the minimum length path, a change of variables from time t to curvilinear abscissa $s(t) = \int_0^t v(u)\, du$ is made. Then, the dynamics can be rewritten as:

$$\begin{cases} x' = \dfrac{dx}{ds} = \cos\gamma\cos\chi, \\ y' = \dfrac{dy}{ds} = \cos\gamma\sin\chi, \\ z' = \dfrac{dz}{ds} = \sin\gamma, \\ \gamma' = \dfrac{d\gamma}{ds} = c(z)\mu, \\ \chi' = \dfrac{d\chi}{ds} = c(z)\dfrac{\eta}{\cos\gamma}, \end{cases} \tag{5}$$

Thus, the dynamics of the forward velocity does not need to be specified in this studies.

3. 3D DUBINS' PATHS IN HETEROGENEOUS ENVIRONMENT

3.1 Problem formulation

Let $\mathbf{x}(s) = (x(s), y(s), z(s), \gamma(s), \chi(s))^\top$ denote a state vector and $\mathbf{u}(s) = (\eta(s), \mu(s))^\top$ denote a control input. The boundary conditions are $\mathbf{x}(0) = \mathbf{x}_0$ and $\mathbf{x}(s_f) = \mathbf{x}_f$ where s_f is the distance from initial state $\mathbf{x}_0$ to goal state $\mathbf{x}_f$. The optimal control problem is to minimize the length of the path by minimizing

$$J(\mathbf{x}_0, \mathbf{x}_f, \mathbf{u}) = \int_0^{s_f} ds \tag{6}$$

In a 2-dimensional plane, it was shown in Dubins (1957) and Boissonnat et al. (1991) that the shortest path between two fixed states of Dubins' vehicle with a constant turning radius is composed of straight line (S) and arc of circle of minimum turning radius (C), *i.e.* CSC or CCC type. In Shkel and Lumelsky (2001), it was proven that CSC type and not CCC type is the shortest path if two states are sufficiently far from each other.

As in 3-dimensional problems, it was proven in Sussmann (1995) that, unlike in a 2-dimensional plane, there can exist a helicoidal arc which is shorter than the CSC path. Thus, the shortest path in 3-dimensional space was a helicoidal arc, a CSC path, a CCC path or a degenerated form of these Dubins' paths. However, in path planning for hypersonic aerial vehicle such as interceptor missile, the target or the mission is known *a priori* using high performance technologies. Therefore, path planning is usually executed between two states that are sufficiently far from each other. As a consequence, in this paper, only the CSC path in a heterogeneous environment using geometric approach is demonstrated with the hypothesis that $\mathbf{x}_0$ and $\mathbf{x}_\mathrm{f}$ are sufficiently far from each other.

In this paper, a 3-dimensional length-optimal path between two given vehicle states for a hypersonic aerial vehicle in a heterogeneous environment, *i.e.* variable turning radius, is considered. In the following sections, first, the Dubins' paths in a heterogeneous environment in a particular 2-dimensional plane are described. Then, the methodology of 3-dimensional path generation is demonstrated.

3.2 Computation of the curve C in a particular 2D plane

In Hérissé and Pepy (2013), the shortest length of Dubins' paths in heterogeneous environments in a 2-dimensional plane, denoted P, where the curvature of the vehicle path decreased exponentially with altitude was demonstrated. Let P denote the plane with a normal vector $\mathbf{b}$ as shown in Fig. 2. The position (x_p, z_p) is associated with vector basis $(\mathbf{e}_\mathrm{p}^1, \mathbf{e}_\mathrm{p}^1)$, of the vehicle on the plane. It can be expressed in $\mathcal{I}$ frame in function of ϕ and ψ as shown in Fig. 2.

In the 2-dimensional system where $\theta_p = \angle(\mathbf{v}, \mathbf{e}_\mathrm{p}^1)$ is a turning angle that, analogously to the original Dubins' paths, shortest paths are a combination of curves of maximum curvature C and straight lines S. Thus, the dynamics of the vehicle can be modeled as:

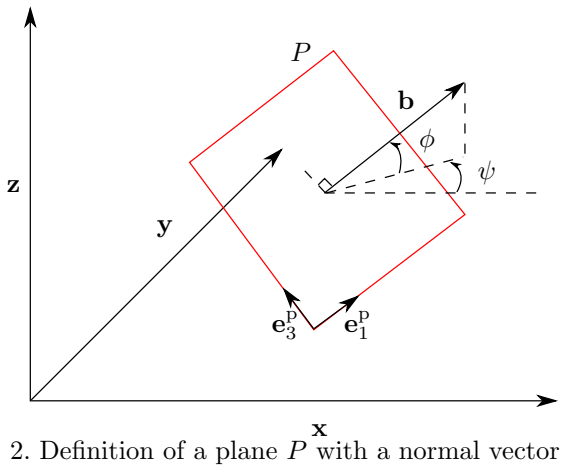

Fig. 2. Definition of a plane P with a normal vector $\mathbf{b}$

$$\begin{aligned} x_p' &= \frac{dx_p}{ds} = \cos\theta_p, \\ z_p' &= \frac{dz_p}{ds} = \sin\theta_p, \\ \theta_p' &= \frac{d\theta_p}{ds} = c(z_p)u_p \ \text{ where } \ u_p \in [-1, 1], \end{aligned} \tag{7}$$

These Dubins' paths have the advantage over the original Dubins' paths in Dubins (1957) and Boissonnat et al. (1991) because they are more realistic for aerial vehicles traveling in a heterogeneous environment.

As a consequence of the calculation on plane P, the environment model, *i.e.* equation (1), on the plane P is rewritten as

$$\rho(z_p) = \rho_0 e^{-z/z_r} = \rho_0 e^{-z_p \cos\phi / z_r}. \tag{8}$$

Moreover, curvature equation (3) can be written as

$$c(z_p) = c_0 e^{-z/z_r} = c_0 e^{-z_p \cos\phi / z_r}. \tag{9}$$

In order to derive the optimal solution with curve of maximum curvature, the magnitude of the control input u_p in system (7) is set to 1. By differentiating θ_p' with respect to s, we obtain

$$\theta_p'' = -\frac{\cos\phi}{z_r}\theta_p' \sin\theta_p. \tag{10}$$

Define $\zeta = \tan\left(\frac{\theta_p}{2}\right)$. After some straightforward trigonometry, we have

$$\cos^2\theta_p = \frac{1-\zeta^2}{1+\zeta^2} \tag{11}$$

$$\theta_p' = 2\frac{\zeta'}{1+\zeta^2} \tag{12}$$

By integrating equation (10) and applying some trigonometric techniques, we have

$$\theta_p' = \frac{\cos\phi}{z_r}\left(\frac{z_r}{\cos\phi}\theta_{p_0}' - \cos\theta_{p_0} + 1 - 2\cos^2\left(\frac{\theta_p}{2}\right)\right) \tag{13}$$

With equations (11), (12) and (13), we obtain

$$\begin{aligned} \zeta' &= A + B\zeta^2, \\ A &= \frac{\cos\phi}{2z_r}\left(\frac{z_r}{\cos\phi}\theta_{p_0}' - \cos\theta_{p_0} + 1\right), \\ B &= A - \frac{\cos\phi}{z_r} \end{aligned} \tag{14}$$

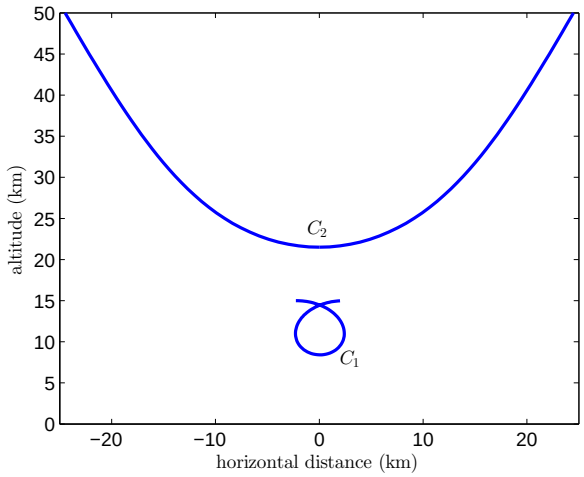

Fig. 3. Examples of arcs of maximum curvature

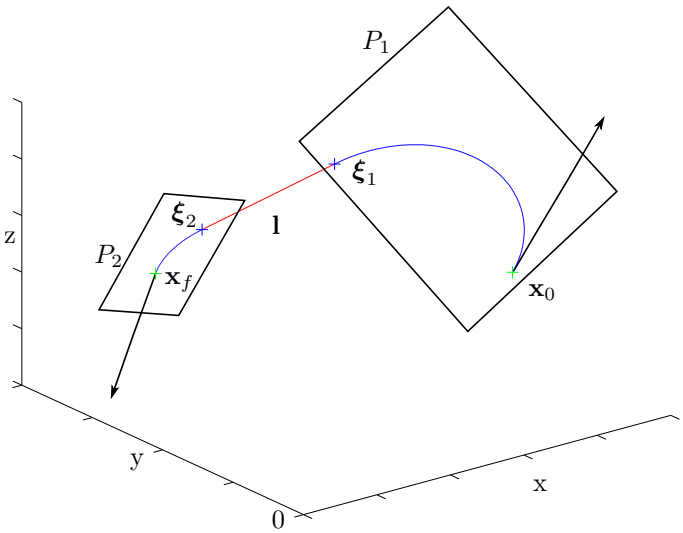

Fig. 4. Example of Dubins' path in 3D

According to system (14), there are four types of curves depending on the values of A and B:

(1) C_1 curve if $AB > 0$,

$$\zeta_1(s) = \sqrt{\frac{A}{B}} \tan\left[A\sqrt{\frac{B}{A}}s + \arctan\left(\sqrt{\frac{B}{A}}\zeta_0\right)\right] \tag{15}$$

The C_1 curve is illustrated in Fig. 3.

(2) C_2 curve if $AB < 0$,

$$\zeta_2(s) = \sqrt{\left|\frac{A}{B}\right|} \tanh\left[A\sqrt{\left|\frac{B}{A}\right|}s + \operatorname{arctanh}\left(\sqrt{\left|\frac{B}{A}\right|}\zeta_0\right)\right] \tag{16}$$

The C_2 curve is also illustrated in Fig. 3. This curve has oblique asymptotes, *i.e.* $\zeta_2 \in \left[-\sqrt{\left|\frac{A}{B}\right|}, \sqrt{\left|\frac{A}{B}\right|}\right]$. This condition must be verified for both ζ_0 and $\zeta_2(s)$. If one or both variables do not respect this condition, there is no solution.

(3) C_3 curve if $A = 0$,

$$\frac{1}{\zeta_3(s)} = \frac{1}{\zeta_0} - Bs \tag{17}$$

(4) C_4 curve if $B = 0$,

$$\zeta_4(s) = \zeta_0 + As \tag{18}$$

Remark 1. C_3 and C_4 curves are the extremal cases of the first two types. They are rarely obtained in reality. Thus, no illustration of these curves is presented in this paper.

θ_p, x_p and z_p can be derived as function of $\zeta(s)$ as follows:

$$\begin{cases} \theta_p(\zeta) = 2\arctan\zeta + k(s)\pi \\ x_p(\zeta) = \dfrac{z_r}{\cos\phi}(\theta_p(\zeta) - \theta_{p_0}) - \dfrac{z_r}{\cos\phi}(A+B)s \\ z_p(\zeta) = \dfrac{z_r}{\cos\phi}\log\left(\dfrac{1+\zeta_0^2}{A+B\zeta_0^2}\dfrac{A+B\zeta^2}{1+\zeta^2}\right) \end{cases} \tag{19}$$

where $k(s)$ is an integer depending on the distance s. In case of C_1 path $k(s)$ is calculated as follows

$$k(s) = \left\lfloor s\sqrt{AB} \Big/ \left(u_p\frac{\pi}{2} - \arctan\left(\sqrt{\frac{B}{A}}\zeta_0\right)\right)\right\rfloor, \quad u_p = \pm 1 \tag{20}$$

where $\lfloor . \rfloor$ is a floor division. Otherwise, $k(s) = 0$ for C_2 type. However, for the optimal solution $k(s)$ value is never greater than 1, *i.e.* $k(s) > 1$ means that the vehicle starts to turn in loop.

3.3 3D paths generation

In order to find the shortest Dubins' path in a heterogeneous environment shown in Fig. 4, let $\mathbf{l} \in \mathbb{R}^3$ denote a line which lies in both plane $P_1$and P_2, *i.e.* $\mathbf{l} \in P_1$ and $\mathbf{l} \in P_2$.

In the following, the cross product of $\mathbf{u}$ and $\mathbf{v}$ is defined by $\mathbf{u} \times \mathbf{v}$. In order to find both curves, the following normal vector to each particular plane P_1 and P_2 must be defined:

- The unit vector perpendicular to the first plane:

$$\mathbf{b}_1 = \frac{\mathbf{l} \times \mathbf{v}_0}{||\mathbf{l} \times \mathbf{v}_0||}; \tag{21}$$

- The unit vector perpendicular to the second plane:

$$\mathbf{b}_2 = \frac{\mathbf{l} \times \mathbf{v}_\mathrm{f}}{||\mathbf{l} \times \mathbf{v}_\mathrm{f}||}; \tag{22}$$

Remark 2. In case $\mathbf{l} \times \mathbf{v}_0 = \mathbf{0}$ or $\mathbf{l} \times \mathbf{v}_\mathrm{f} = \mathbf{0}$, it means that there is no curve. Thus, the CSC type degrades to CS, SC, or S type. However, it is pretty rare to reach this condition.

θ_{p_1} on plane P_1 and θ_{p_2} on plane P_2 in equation (19) are defined as follows

$$\theta_{p_1} = \angle(\mathbf{l}, \mathbf{e}_1^{p_1}) \tag{23}$$

$$\theta_{p_2} = \angle(\mathbf{l}, \mathbf{e}_1^{p_2}) \tag{24}$$

Then, the position of $\boldsymbol{\xi}_1$ on plane P_1 and $\boldsymbol{\xi}_2$ on plane P_2 can be found using the calculation shown in Section 3.2. Then, $\boldsymbol{\xi}_1 = (x_1, y_1, z_1)$ and $\boldsymbol{\xi}_2 = (x_2, y_2, z_2)$ in $\mathcal{I}$ frame can be found as follows:

$$\begin{cases} x_1 = -z_{p_1}\sin\phi_1\cos\psi_1 - x_{p_1}\sin\psi_1 + x_0 \\ y_1 = -z_{p_1}\sin\phi_1\sin\psi_1 + x_{p_1}\cos\psi_1 + y_0 \\ z_1 = z_{p_1}\cos\phi_1 + z_0 \end{cases} \tag{25}$$

$$\begin{cases} x_2 = -z_{p_2}\sin\phi_2\cos\psi_2 - x_{p_2}\sin\psi_2 + x_f \\ y_2 = -z_{p_2}\sin\phi_2\sin\psi_2 + x_{p_2}\cos\psi_2 + y_f \\ z_2 = z_{p_2}\cos\phi_2 + z_f \end{cases} \tag{26}$$

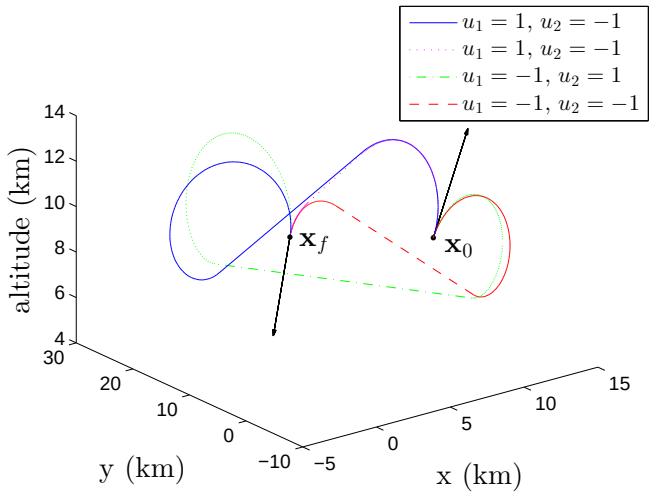

Fig. 5. Four possible CSC paths between two states

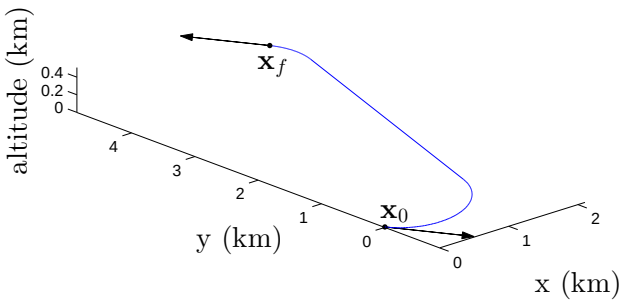

Fig. 6. Case 1: $\mathbf{x}_0 = (0, 0, 0.005, 0, -\pi/3)^\top$ and $\mathbf{x}_f = (2, 4, 0.5, 0, 2\pi/3)^\top$

Recall that both curves are obtained by considering $(x_p, z_p) = (0, 0)$ as a origin and (ϕ_1, ψ_1) and (ϕ_2, ψ_2) as orientations of $\mathbf{b}_1$ and $\mathbf{b}_2$, respectively.

The orientations $\mathbf{v}_1$ and $\mathbf{v}_2$ can be found by rotating $\mathbf{v}_0$ and $\mathbf{v}_\mathrm{f}$ by $\Delta\theta_1 = \theta_{p_1} - \theta_{p_0}$ and $\Delta\theta_2 = \theta_{p_2} - \theta_{p_f}$ around vectors $\mathbf{b}_1$ and $\mathbf{b}_2$, respectively. We have

$$\mathbf{v}_1 = R_{b_1}\mathbf{v}_0 \tag{27}$$
$$R_{b_1} = \cos\Delta\theta_1\mathbf{I}_3 + \sin\Delta\theta_1\mathbf{C}_1 + (1-\cos\Delta\theta_1)\mathbf{D}_1 \tag{28}$$
$$\mathbf{v}_2 = R_{b_2}\mathbf{v}_\mathrm{f} \tag{29}$$
$$R_{b_2} = \cos\Delta\theta_2\mathbf{I}_3 + \sin\Delta\theta_2\mathbf{C}_2 + (1-\cos\Delta\theta_2)\mathbf{D}_2 \tag{30}$$

where $\mathbf{I}_3$ is an identity matrix of order 3. $\mathbf{C}_1$, $\mathbf{D}_1$, $\mathbf{C}_2$, and $\mathbf{D}_2$ are defined as follows:

$$\mathbf{C}_1 = \begin{bmatrix} 0 & -b_{1_z} & b_{1_y} \\ b_{1_z} & 0 & -b_{1_x} \\ -b_{1_y} & b_{1_x} & 0 \end{bmatrix}$$
$$\mathbf{D}_1 = \begin{bmatrix} b_{1_x}^2 & b_{1_x}b_{1_y} & b_{1_x}b_{1_z} \\ b_{1_x}b_{1_y} & b_{1_y}^2 & b_{1_y}b_{1_z} \\ b_{1_x}b_{1_z} & b_{1_y}b_{1_z} & b_{1_z}^2 \end{bmatrix}$$
$$\mathbf{C}_2 = \begin{bmatrix} 0 & -b_{2_z} & b_{2_y} \\ b_{2_z} & 0 & -b_{2_x} \\ -b_{2_y} & b_{2_x} & 0 \end{bmatrix}$$
$$\mathbf{D}_2 = \begin{bmatrix} b_{2_x}^2 & b_{2_x}b_{2_y} & b_{2_x}b_{2_z} \\ b_{2_x}b_{2_y} & b_{2_y}^2 & b_{2_y}b_{2_z} \\ b_{2_x}b_{2_z} & b_{2_y}b_{2_z} & b_{2_z}^2 \end{bmatrix}$$

Once two curves have been found, a solver is used to find $\mathbf{l}$ by verifying the objective function $F(\mathbf{l}) = \mathbf{l} - (\boldsymbol{\xi}_2 - \boldsymbol{\xi}_1) = \mathbf{0}$. Thus, a line, which is on both plane P_1 and plane P_2, connecting both curves is found.

Remark 3. With this methodology, the conditions $\mathbf{l}\times\mathbf{v}_1 = \mathbf{0}$ and $\mathbf{l}\times\mathbf{v}_2 = \mathbf{0}$ are automatically verified.

There can exist four types of CSC paths shown in Fig. 5 where $u_p = \pm 1$ for both curves. The solutions can be found in the same way as the demonstration. Among these paths, the shortest Dubins' path is chosen.

4. SIMULATION RESULTS

Simulations are generated in several case studies. Each state is presented by $\mathbf{x} = (x, y, z, \gamma, \chi)^\top$ in Table 1 for each case. According to the standard air density at the sea level, the maximum curvature of the vehicle path at sea level $c_0 = 1.4 \times 10^{-3}\mathrm{m}^{-1}$ and the reference altitude $z_r = 7500\mathrm{m}$ are chosen to simulate the results in this paper. In the following figures, the trajectory presented in blue curve starts at $\mathbf{x}_0$ and arrives at $\mathbf{x}_f$. The arrows represent the orientation of each state.

Case 1 represents a scenario where the maximum curvature of the vehicle path does not vary much. The maximum curvature at $\mathbf{x}_0$ is $1.4 \times 10^{-3}\,(\mathrm{m}^{-1})$ and the maximum curvature at $\mathbf{x}_f$ is $1.3 \times 10^{-3}\,(\mathrm{m}^{-1})$. The simulated trajectory is shown in Fig. 6. In this case, the calculation in Hota and Ghose (2010) is still valid because the curvature can be considered constant. In the following cases, the difference between maximum curvature at both states is gradually increased. Thus, the trajectories calculated using vehicle model in Hota and Ghose (2010) become very difficult to follow by the real vehicle. The simulated results are shown in Fig. 7 and 8. In case 2, the maximum curvature at $\mathbf{x}_0$ is $3.69 \times 10^{-4}\,(\mathrm{m}^{-1})$ and the maximum curvature at $\mathbf{x}_f$ is $4.96 \times 10^{-5}\,(\mathrm{m}^{-1})$. In case 3, the maximum curvature at $\mathbf{x}_0$ is $7.19 \times 10^{-4}\,(\mathrm{m}^{-1})$ and the maximum curvature at $\mathbf{x}_f$ is $4.97 \times 10^{-5}\,(\mathrm{m}^{-1})$.

As we can see from the simulated results that the trajectories become more realistic for the aerial vehicle to follow according to the vehicle model. Moreover, the computational time is less than 1 second to find each trajectory. The simulations are run in MATLAB2012a in a intel xeon 2.8GHz processor with 8 GB RAM.

5. CONCLUSION AND PERSPECTIVES

The optimal path generation in 3-dimensional space is the key element in most of planning algorithms especially in the aeronautics domain. The optimal path in a heterogeneous environment developed based on geometrical approach is very efficient and fast to generate. The path

Table 1. Boundary conditions and results for simulations

Case study	$\mathbf{x}_0$ (km,km,km,radian,radian)	$\mathbf{x}_f$ (km,km,km,radian,radian)	3D Dubins' path length (km)
Case 1	$(0, 0, 0.005, 0, -\pi/3)$	$(2, 4, 0.5, 0, 2\pi/3)$	5.65
Case 2	$(0, 0, 10, \pi/12, \pi/12)$	$(20, 15, 25, 0, -2\pi/3)$	59.84
Case 3	$(0, 0, 5, \pi/2, 5\pi/6)$	$(15, 15, 25, -\pi/12, \pi/3)$	37.04

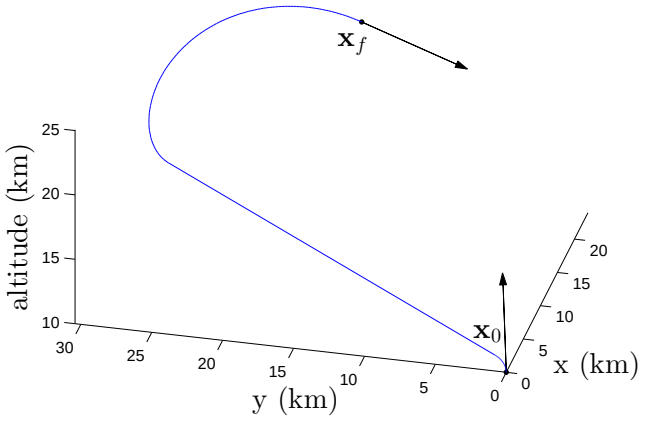

Fig. 7. Case 2: $\mathbf{x}_0 = (0, 0, 10, \pi/12, \pi/12)^\top$ and $\mathbf{x}_f = (20, 15, 25, 0, 4\pi/3)^\top$

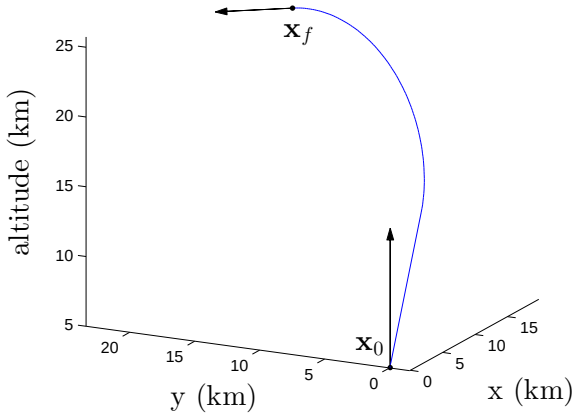

Fig. 8. Case 3: $\mathbf{x}_0 = (0, 0, 5, \pi/2, 5\pi/6)^\top$ and $\mathbf{x}_f = (15, 15, 25, -\pi/12, \pi/3)^\top$

obtained by this method is more realistic than path generated by existing Dubins' paths.

This method is computationally fast and easy to implement. Moreover, it can give the shortest and more realistic path from the starting to the ending state. Therefore, it can be applied to many applications such as path planning in complex environment in Pharpatara et al. (2013). However, the path generation can be improved by finding a shortest path of helicoidal arc type between two states that are relatively close to each other so that the path generation can cover all cases in 3-dimensional space.

REFERENCES

Boissonnat, J.D., Cérézo, A., and Leblond, J. (1991). Shortest paths of bounded curvature in the plane. Technical report, Institut National de Recherche en Informatique et en Automatique.

Dolinskaya, I.S. and Maggiar, A. (2012). Time-optimal trajectories with bounded curvature in anisotropic medium. *The International Journal of Robotics Research*, 14(31), 1761–1793.

Dubins, L.E. (1957). On curves of minimal length with a constraint on average curvature and with presribed initial and terminal position and tangents. *American Journal of Mathematics*, 79, 497–516.

Hérissé, B. and Pepy, R. (2013). Shortest paths for the dubins' vehicle in heterogeneous environments. *In Proceedings of the IEEE Conference on Decision and Control*, 4504–4509.

Hota, S. and Ghose, D. (2010). Optimal path planning for an aerial vehicle in 3d space. *IEEE Conference on Decision and Control*, 4902–4907.

Hota, S. and Ghose, D. (2014). Optimal trajectory planning for unmanned aerial vehicles in three-dimensional space. *Journal of aircraft*, 51(2), 681–687.

McGee, T.G., Spry, S., and Hedrick, J.K. (2005). Optimal path planning in a constant wind with a bounded turning rate. *In Proceedings of the AIAA Guidance, Navigation, and Control Conference and Exhibit*, 1–11.

Pharpatara, P., Pepy, R., Hérissé, B., and Bestaoui, Y. (2013). Missile trajectory shaping using sampling-based path planning. In *the IEEE/RCJ International Conference on Intelligent Robots and Systems*, 2533–2538. Tokyo, Japan.

Reeds, J.A. and Shepp, L.A. (1990). Optimal paths for a car that goes both forwards and backwards. *Pacific Journal of Mathematics*, 145, 367–393.

Sanfelice, R. and Frazzoli, E. (2008). On the optimality of dubins paths across heterogeneous terrain. *Hybrid Ssytems: Computationa and Control*, 457–470.

Shanmugavel, M. (2007). *Path planning of multiple autonomous vehicles*. Ph.D. thesis, Cranfield University.

Shkel, A.M. and Lumelsky, V. (2001). Classification of the dubins set. *Robotics and Autonomous Systems*, 34, 179–202.

Sussmann, H.J. (1995). Shortest 3-dimensional paths with prescribed curvature bound. *IEEE Conference on Decision and Control*, 4, 3306–3312.